JOURNAL OF MAGNETIC RESONANCE **130,** 18–26 (1998)
ARTICLE NO. MN971284

^{2}H NMR Time Domain Analysis of Ultraslow Reorientations in Supercooled Liquids

B. Geil,* F. Fujara,* and H. Sillescu†

*Fachbereich Physik, Universität Dortmund, D-44221 Dortmund, Germany; and †Institut für Physikalische Chemie, Universität Mainz, D-55099 Mainz, Germany

Received May 9, 1997; revised August 20, 1997

A method for evaluating ^{2}H NMR stimulated echo experiments in the time domain is presented. It exhibits a high sensitivity to molecular reorientation mechanisms for small angles. Reorientations with jump angles below 25° can be resolved with a precision of ≈1° so that, e.g., rotational diffusion and finite jump angle mechanisms become distinguishable. The method, applicable to isotropic reorientation models, is thought to extend the domain of 2D exchange spectroscopy where the best resolution is obtained in the large angle range of anisotropic reorientational mechanisms. Application to reorientation in the supercooled melt of *ortho*-terphenyl is presented. These data clearly show that the molecular reorientation of *ortho*-terphenyl molecules cannot be described by small angular step rotational diffusion. A better parametrization of the experimental data incorporates elementary jump angles in the range of approximately 10°.

INTRODUCTION

The success of two-dimensional exchange spectroscopy in analyzing slow molecular motion in solids (*1*) has resulted in a certain neglect of time domain techniques. However, since the primary NMR signals are obtained in the time domain and Fourier transformation may imply systematic errors it should not be surprising to find situations in which the analysis of time domain signals is advantageous and yields more information on details of molecular reorientation than that of conventional 2D spectroscopy.

Instead of recording (and Fourier transforming) the whole shape of the NMR echoes (*1, 2*) the time domain analysis concentrates on the amplitude of the echo maximium. In case of the stimulated NMR echo, used in our experiments as well as in 2D exchange spectroscopy, the echo amplitude is a function of two experimentally adjustable times, τ, the evolution time and t, the mixing time (cf. Fig. 1). The evolution time τ turns out to be a parameter which serves as a filter for the sensitivity of the experiment on the size of the reorientation angles: with increasing values of τ the stimulated echo experiment gets more and more sensitive to smaller reorientation angles. The mixing time t is the dynamical variable of the stimulated echo experiment, the time over which the molecular reorientation is correlated. In the method described below, we will record the decay of the stimulated echo amplitude (for several fixed values of τ) as a function of t. The time scale of these decays is mainly dominated by the time scale of the molecular reorientation but also depends on the value of the evolution period τ. It is just this τ dependence which is related to the geometry of the reorientation process. The aim of the method presented is to reduce the amount of information obtained from the shape of the decay curves to a few τ-dependent parameters which can easily be compared with theoretical results obtained from simulations of different reorientation models.

Although most of the theoretical background of our time domain analysis can be found in the monograph by Schmidt-Rohr and Spiess (*1*) we provide the relevant definitions and equations for the convenience of the reader in the following sections where the main advantages over 2D spectroscopy are also demonstrated (see Figs. 2, 3, and 5). A detailed analysis of an example, namely, molecular reorientation in supercooled deuterated *ortho*-terphenyl is discussed in the experimental section. It should be noted that parts of the results have already been published in Ref. (*3*). A general review of molecular dynamics above and close to the glass transition can be found in Ref. (*4*).

THEORY

The stimulated echo following the three-pulse sequence shown in Fig. 1 can be formulated as

$$S(\tau, t, \tilde{\tau}) = \langle e^{-i\tau\omega_Q(0)} e^{i\tilde{\tau}\omega_Q(t)} \rangle \qquad [1]$$

$$\omega_Q(t) = \pm \frac{\delta}{2} (3\cos^2\beta(t) - 1), \qquad [2]$$

where $2\delta = 3e^2Qq/4\hbar$ is the nuclear quadrupole splitting in case of ^{2}H NMR. In deuterated organic compounds where the quadrupole coupling tensor is axially symmetric with its main axis parallel to the bond direction the angle β is the angle between the C–D bond and the magnetic field $\mathbf{B}_0$. By

1090-7807/98 $25.00

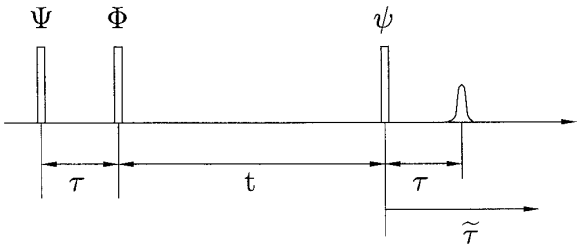

FIG. 1. The pulse sequence of the stimulated echo experiment. Choosing $\Psi = 90^\circ_y$, $\Phi = 45^\circ_x$, and $\psi = 45^\circ_x$ one obtains the pure sin–sin correlation function while $\Psi = 90^\circ_y$, $\Phi = 90^\circ_y$, and $\psi = 90^\circ_y$ leads to the pure cos–cos correlation function.

setting appropriate RF phases one can separately determine the cosine and sine parts of the correlation function (Eq. [1]):

$$S_{\cos}(\tau, t, \tilde{\tau}) = \langle \cos \tau\omega_Q(0) \cos \tilde{\tau}\omega_Q(t) \rangle$$
$$S_{\sin}(\tau, t, \tilde{\tau}) = \langle \sin \tau\omega_Q(0) \sin \tilde{\tau}\omega_Q(t) \rangle. \quad [3]$$

By rewriting the ensemble average $\langle \cdots \rangle$ of Eq. [1] as

$$S(\tau, t, \tilde{\tau}) = \int d\omega_1 \int d\omega_2 \exp(-i\tau\omega_1) \times \exp(i\tilde{\tau}\omega_2) \tilde{P}_{2,0}(\omega_1, 0; \omega_2, t), \quad [4]$$

where $\omega_1 = \omega_Q(0)$, $\omega_2 = \omega_Q(t)$, and $\tilde{P}_{2,0}(\omega_1, 0; \omega_2, t)$ is the joint probability of finding a single spin at frequency ω_1 at the beginning *and* at ω_2 at the end of the mixing period t, one recognizes in Eq. [4] the 2D Fourier transform leading to 2D exchange spectroscopy. In a time domain analysis it is most convenient to focus on the echo maximum at $\tilde{\tau} = \tau$ and to analyze $S(\tau, t) = S(\tau, t, \tilde{\tau} = \tau)$ in terms of

$$P_{2,0}(\beta_1, 0; \beta_2, t) = 3\delta^2 \left[\left(1 \pm \frac{2\omega_1}{\delta}\right)\left(1 \pm \frac{2\omega_2}{\delta}\right) \times (1 - \cos^2\beta_1)(1 - \cos^2\beta_2) \right]^{1/2} \times \tilde{P}_{2,0}(\omega_1, 0; \omega_2, t) \quad [5]$$

with β_1 and β_2 being the orientation angles of a C–D bond relative to the $\mathbf{B}_0$ field at times $t = 0$ and t. If one introduces the reorientation angle β connecting the C–D bond directions at $t = 0$ and t, respectively, one can introduce the reorientation angle distribution (RAD) $P_{1,1}(\beta, t|0, 0)$ by the expression

$$P_{2,0}(\beta_1, 0; \beta_2, t) = \int d\beta P_{2,1}(\beta_2, t; \beta_1, 0|\beta, t) \cdot P_{1,1}(\beta, t|0, 0). \quad [6]$$

Here $P_{2,1}(\beta_2, t; \beta_1, 0|\beta, t)$ is the probability of finding a C–D bond orientated at the angle β_1 initially and at the angle β_2 after the mixing period under the condition that the reorientation in the mixing period was β.

With this decomposition of the probabilities one is able to perform the integrations over β_1 and β_2 and the correlation function (Eq. [4]) simplifies to (*5, 6*)

$$S(\tau, t, \tilde{\tau}) = \int d\beta K(\tau, \beta) \cdot P_{1,1}(\beta, t|0, 0). \quad [7]$$

It is worthwhile to note that the introduced ''integral kernel''

$$K(\tau, \beta) := \int d\beta_1 \int d\beta_2 e^{-i\tau\omega(\beta_1)} e^{i\tau\omega(\beta_2)} \times P_{2,1}(\beta_2, t; \beta_1, 0|\beta, t) \quad [8]$$

does not depend on any properties of the dynamical model and contains only the characteristics of the spectroscopic method under consideration. On the other hand the complete information on the dynamics of the system is encoded in the RAD $P_{1,1}(\beta, t|0, 0)$. With the knowledge of the complete time evolution $P_{1,1}(\beta, t|0, 0)$ one can calculate the stimulated echo experiment. From Eq. [7] it is obvious that the time dependent RAD is convoluted with the integral kernel $K(\tau, \beta)$. In other words, $K(\tau, \beta)$ acts as a filter on $P_{1|1}(\beta, t|0, 0)$ using the evolution time τ as an adjustable parameter to change the sensitivity on different values of β. Thus for small values of τ the stimulated echo experiment is sensitive on all values of β while with increasing τ the experiments become more and more sensitive on smaller β values. Since in most cases one would not be able to calculate this time evolution of the RAD analytically we use the following general numerical approach:

The range of the stochastic variables β_1 and β_2 ($\beta_1, \beta_2 \in [0, \pi]$) is divided into N intervals of width $\Delta\beta = \pi/N$ so that $\beta_{1,2}(n_i) = (n_i - 1/2)\Delta\beta$. The joint probability function $P_{2,0}(\beta_2, t; \beta_1, 0)$ is then converted into a square $N \times N$ matrix $P_{2,0}(n_2, t; n_1, 0) =: \underline{\underline{P}}(t)$.

The time evolution of this probability matrix obeys the master equation

$$\frac{\partial}{\partial t} \underline{\underline{P}}(t) = \underline{\underline{\Gamma}}\,\underline{\underline{P}}(t) \quad [9]$$

with $\underline{\underline{\Gamma}}$ being the so-called *exchange matrix*. The off-diagonal elements $\Gamma_{k,l}$ are the transition rates from site k to site l, and the diagonal elements $\Gamma_{k,k}$ are the sums over all off-diagonal elements in the kth row. This set of coupled linear differential equations can be solved via matrix algebra (*7*). Finally the RAD can be found to be (*8*)

$$P_{1,1}(\beta, t|0, 0) = \lim_{\beta_1 \to 0} \frac{P_{2,0}(\beta_1, \beta_2 = \beta; t)}{P_{1,0}(\beta_1)}. \quad [10]$$

In the frame of this work we will consider three different models for the reorientation dynamics:

• *Isotropic rotational diffusion* (IRD): The orientation vector of a C–D bond performs a diffusional Brownian motion on the surface of a sphere, and the time evolution of the RAD is given by the solution of the diffusion equation in spherical coordinates (*9, 10*). The equations of motion for the joint probability $P_{2,0}$ could have been solved analytically, but we prefered to use the above numerical way, allowing us to use the same computational algorithms within all the models. The off-diagonal elements of the (tridiagonal) exchange matrix were found to be (*1*)

$$\Gamma^{\mathrm{IRD}}_{m,m+1} = \frac{D}{\Delta\beta^2} \frac{\sin(m\Delta\beta)}{\sin\left(\left(m + \frac{1}{2}\right)\Delta\beta\right)} \qquad [11]$$

and

$$\Gamma^{\mathrm{IRD}}_{m+1,m} = \frac{D}{\Delta\beta^2} \frac{\sin(m\Delta\beta)}{\sin\left(\left(m - \frac{1}{2}\right)\Delta\beta\right)}. \qquad [12]$$

• *Isotropic random jumps* (IRJ). Here the orientation vector of a C–D bond is allowed to jump with equal probabilities from any initial position into any other position. Again this model can be solved analytically, but we use (*1*)

$$\Gamma^{\mathrm{IRJ}}_{l,k} = \frac{1}{\tau_c} P_{1,0}((l - 1/2)\Delta\beta), \qquad [13]$$

with τ_c being the correlation time of this model.

• *Isotropic finite angle jump* (IFJ). The elementary step of this model is a reorientational jump in arbitrary direction but with a well-defined jump angle (*5*). Thus, after one elementary jump a C–D bond can be found with equal probabilities on a cone with twice the elementary jump angle around the initial position of the C–D bond. With α being the *elementary jump angle size* which is an adjustable parameter, this model is much more flexible than the two former ones. Especially in the limit $\alpha \to 0°$ this model is nothing else than the *isotropic rotational diffusion.* If $\beta_1 = k \cdot \Delta\beta$ and $\beta_2 = l \cdot \Delta\beta$, the elements of the exchange matrix for this model are found to be

$$\Gamma^{\mathrm{IFJ}}_{k,l} = \Phi\left(\beta_1, \beta_2 + \frac{1}{2}\Delta\beta\right) - \Phi\left(\beta_1, \beta_2 - \frac{1}{2}\Delta\beta\right) \qquad [14]$$

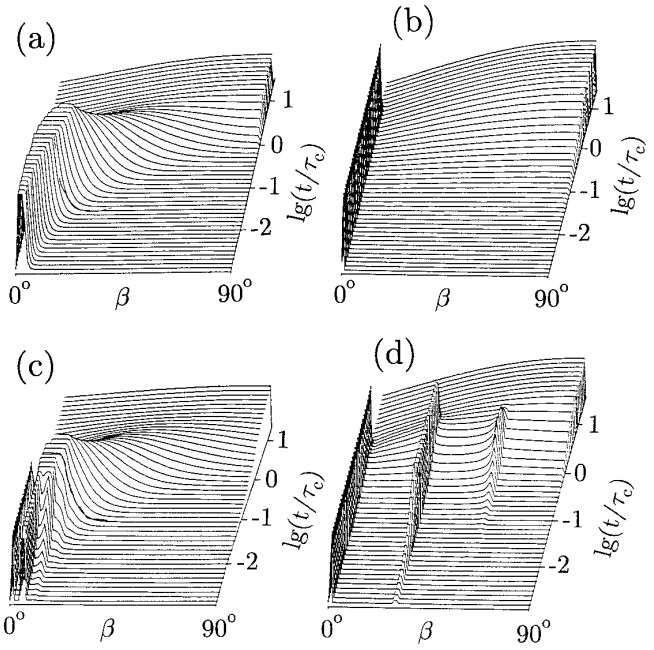

FIG. 2. The time evolution of the RAD for several models of reorientation dynamics: (a) isotropic reorientational diffusion (IRD), (b) isotropic random jump (IRJ), (c) isotropic finite angle jump (IFJ) with $\alpha = 5°$, and (d) IFJ with $\alpha = 30°$. In all cases the initial distribution was a delta function at $\beta_3 = 0°$ and all models end up in the same ''isotropic final state.'' Note the truncation of the initial peak at t/τ_c values below approximately 1 which is necessary to demonstrate the long-time behavior of the RAD with small intensities in the large angle regime.

with

$$\Phi(\beta_1, \beta_2) = \arccos\left[\frac{\cos(\beta_2) - \cos(\beta_1)\cos(\alpha)}{\sin(\beta_1)\sin(\alpha)}\right]. \qquad [15]$$

For each of these models the time evolution of the corresponding RAD was calculated from Eq. [10]. The results for some of these models are shown in Fig. 2. Note that in this figure the mixing period *t* is normalized to the correlation time τ_c of the model and is drawn on a logarithmic scale. In all of these RADs the time scale for the evolution from the original delta function at $t = 0$, $\beta = 0$ to an identical isotropic final state (equilibrium distribution) covers more than four decades.

DATA ANALYSIS IN THE TIME DOMAIN

Keeping in mind that the RAD contains the whole information about the mechanism of reorientational motion, one can state that two different models of motion can *only* be distinguished *if* the time evolutions of the corresponding RADs are distinguishable. In contrast to *N*-site jump models (like phenyl ring flips or tetrahedral jumps) where the mechanism of motion is easily determined by the characteristic

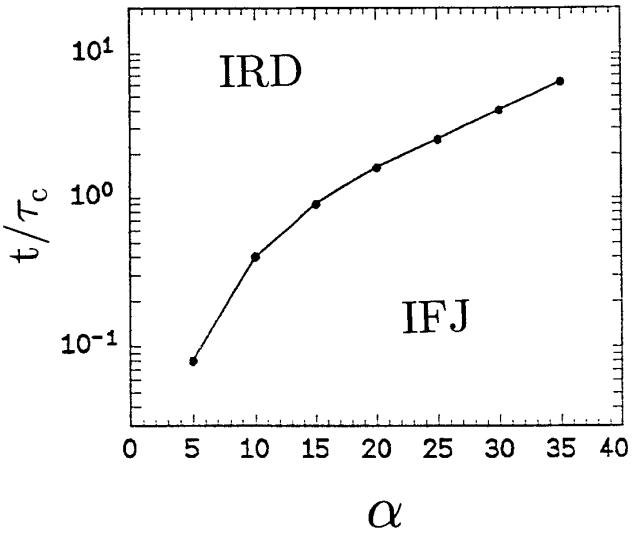

FIG. 3. An estimation of the boundary where 2D exchange spectra can resolve small angle reorientations. For mixing times above this boundary the RAD of small angle IFJ models cannot be distinguished from the IRD model. Thus, in this upper time regime all 2D exchange spectra can be interpreted in terms of an IRD model.

final state in 2D spectra, here, in the case of isotropic reorientation models with $N \to \infty$, one must focus on the ''path'' along which the final state is reached. To this end one should measure the complete time evolution of the RAD (cf. Fig. 2) in a more or less direct way.

Analyzing the RADs—especially those for small angle reorientiations—a main disadvantage of 2D spectroscopy is obvious: A single 2D spectrum is completely determined by a single line (t = const) of the RAD. At short times the main intensity of the RAD is still contained in the delta peak at the origin, leading to a dominating diagonal Pake pattern in the spectrum. Please note the cut-off along the z axis visible in the initial peak in Fig. 2 up to t/τ_c-values of approximately 1. In these plots we introduced that cutoff to stress the characteristic long-time evolution with small intensities in the large angle regime. At longer mixing times, when the delta peak in the RAD gets weaker, the background pattern in the RAD gets more and more similar to that of *isotropic rotational diffusion* (cf. Figs. 2a and 2c). Therefore, in the case of small angle reorientation the time scale where 2D spectroscopy leads to resolved motional patterns might become *very* short, and it should be the aim to bundle this background intensity which is distributed over the whole ω_1, ω_2 plane in 2D spectroscopy. In Fig. 3 we show an estimation of the limit $t_{\max}$ as a function of the elementary jump angle α: The RAD and a single 2D spectrum of a finite angle jump model cannot be distinguished from IRD if the mixing period t exceeds that boundary value $t_{\max}$. $t_{\max}$ was estimated by comparing the RAD of the IFJ model with the RAD of the IRD model at the same value of the normalized mixing time t/τ_c. Two RADs are considered to be undistinguishable if the deviations are below $\approx$1% for all values of β. Note that there is also a lower limit of the mixing period t given by some details of the stimulated echo experiment: The simple correlation function (Eq. [1]) describing the echo amplitude only holds if the mixing period t is large compared to the evolution time τ.

To avoid these difficulties we introduce the mixing period t to be our main dynamical variable (in 2D spectroscopy the continuously recorded time variable is the period $\tilde{\tau}$ after the third pulse which contains only redundant information on the mechanism of the reorientation). Measuring the decay of the stimulated echo amplitude with a high density of points (equidistant on a logarithmic scale) over a wide range of t values and repeating these measurements for several (linearly incremented) values of the evolution period τ, one obtains a two-dimensional set of data corresponding to the two-dimensional representation of the RAD in Fig. 2. If one was able to invert Eq. [7], one could directly transform the τ axis of these 2D data sheets into the β axis of the time evolution of the RAD and one would gain the complete information on the reorientation mechanism. However, this task is as difficult as transforming a 2D spectrum into the corresponding RAD, and other ways of comparing the 2D data sheets with reorientation mechanisms must be chosen.

First, it is convenient to reduce the dimensionality of the data sheets. Comparing experimental data with several simulated curves can be performed more easily if one must only deal with one-dimensional data. In our analysis we tried to eliminate the t-dependence of the two-dimensional data by parameterizing the individual decay curves via a stretched exponential function (Kohlrausch–Williams–Watts (KWW) function (*11, 12*)):

$$S(\tau, t) \propto \exp\left[-\left(\frac{t}{\tau_k(\tau)} \right)^{\beta_k(\tau)} \right]. \qquad [16]$$

In general the t-dependent echo decay curves are strongly nonexponential and the stretched exponential ansatz is used here to smoothly fit the experimental data. An integration of the t-dependent decays, leading to a well-defined mean decay time $\langle \tau_k \rangle$, can then be performed analytically with the obtained KWW functions

$$\langle \tau_k \rangle = \int_0^\infty dt S(\tau, t) = \tau_k \cdot \beta_k^{-1} \Gamma(\beta_k^{-1}) \qquad [17]$$

with the gamma function $\Gamma(x)$. From this point of view the KWW fits are only used to avoid problems in integrating noisy experimental data. In order to obtain comparable parameters for the simulated reorientation models the simulated decay curves have been treated in the same manner. Please note that it is not too important for the data evaluation described below if the stretched exponential function does

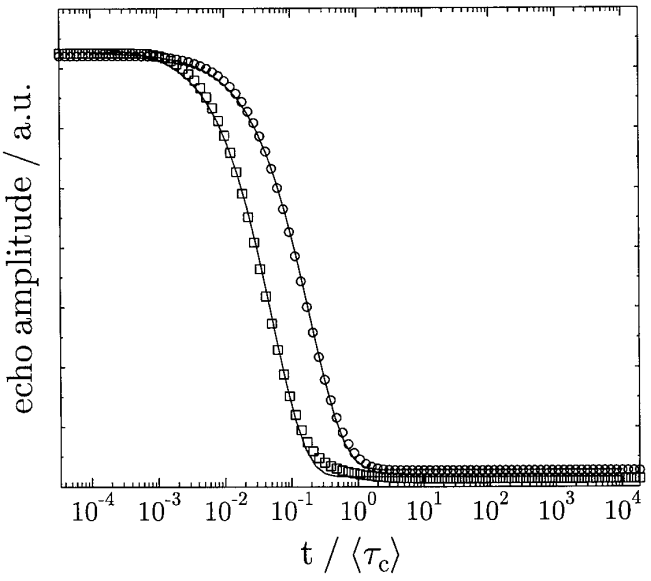

FIG. 4. The fitting of simulated echo decay curves with the KWW function (Eq. [16]). The simulations were performed for the IFJ model with $\alpha = 10°$ and a distribution of correlation times according to Eq. [18] with a decadic full-width at half-maximum (Eq. [20]) of $\sigma_{dec} = 0.5$. The mixing period t is normalized to the mean value $\langle\tau_c\rangle$ (Eq. [19]) of this correlation time distribution. The circles and squares represent the simulated decay curves for $\tau = 6$ μs and $\tau = 40$ μs, respectively, while the solid lines show the obtained KWW functions (with values of $\beta_k \approx 0.8$).

not describe our data very well. As long as the experimental data and simulated decay curves are treated in the same way, and as long as we do not try to interpret the two parameters $\langle\tau_k\rangle$ and β_k in terms of physics, we can compare the experimental with the simulated results.

In Fig. 4 the fitting of two simulated echo decay curves is shown. These simulations have been performed with parameters representative of the IFJ models used in the evaluation of our data as discussed in the experimental section. Regarding these plots, it is obvious that the rough shape of the stimulated echo decay curves can be described via KWW functions but there are also systematic deviations in the range of strong curvatures at very short and very long decay times.

The two parameters $\langle\tau_k\rangle$ and β_k still depend on the evolution time τ. Since τ is directly connected with the sensitivity of the stimulated echo experiment on the reorientation angle β, the τ dependence of both parameters is expected to depend on the size of the elementary jump angle characterizing the mechanism of molecular reorientation.

Figure 5 shows the results for some simulated IFJ models where the elementary jump angle is varied in the small angle range. The simulations, based on Eqs. [7] to [15], were performed using 90×90 exchange matrices with a resolution of 1° and a quadrupole coupling constant of 182.5 kHz (corresponding to that of *ortho*-terphenyl used in our experiments). In contrast to the 2D spectrum analysis this method turns out to be highly sensitive to small angle ($\alpha < 25°$) reorientations. The characteristic τ dependence of both parameters, $\langle\tau_k\rangle$ (Fig. 5a) as well as β_k (Fig. 5b) strongly depends on the size of the elementary jump angle. This gives us an additional cross check, since the comparison of experimental data with simulated curves must simultaneously fit to both parts of Fig. 5. Note that the oscillatory behavior of both parameters originates from the τ-dependent oscillations of $S_{cos}(\tau, t, \tilde{\tau})$ or $S_{sin}(\tau, t, \tilde{\tau})$ (cf. Eq. [3] and Fig. 6). It is highly sensitive to the quadrupole coupling constant of the system and depends on the type of the correlation function (sin−sin or cos−cos) used to perform the experiments.

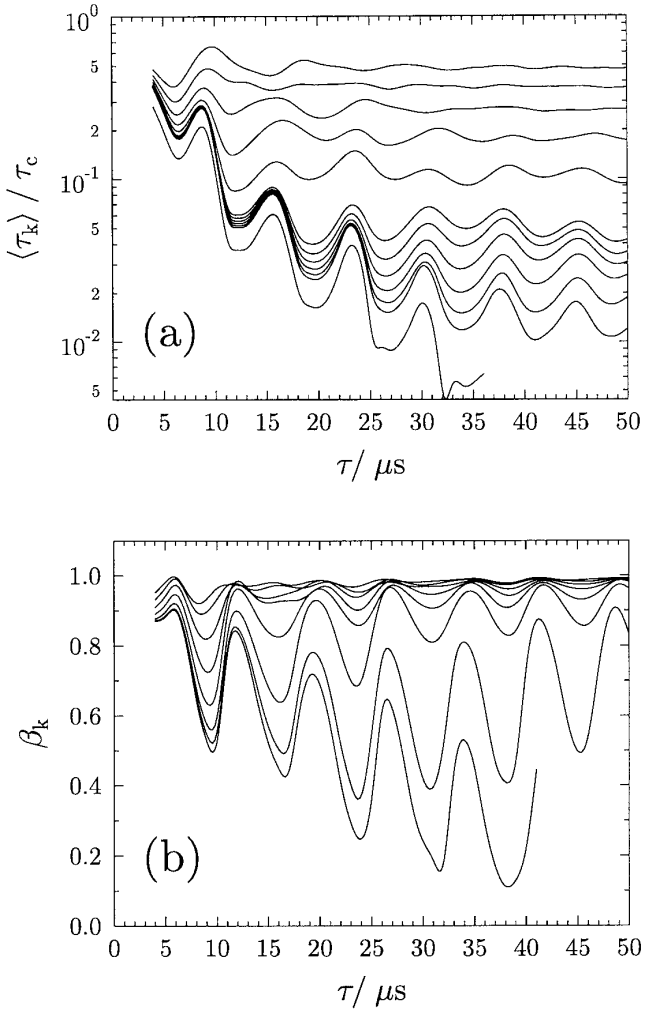

FIG. 5. The τ dependence of the parameters $\langle\tau_k\rangle$ (a) and β_k (b) for the IFJ model and various values of the elementary jump angle (from bottom to top: (a) $\alpha = 1°, 5°, 6°, 7°, 8°, 9°, 10°, 15°, 20°, 25°, 30°, 35°$; (b) $\alpha = 1°, 5°, 10°, 15°, 20°, 25°, 30°, 35°$). The curves were obtained by fitting simulated cos−cos correlation functions (using the quadrupole coupling constant of *ortho*-terphenyl, 182.5 kHz) with Eqs. [16] and [17].

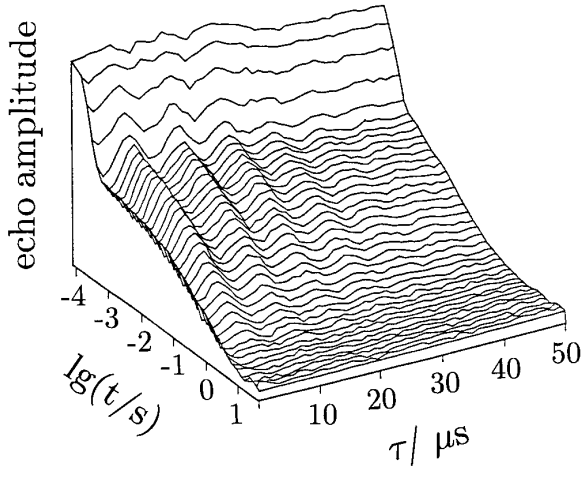

FIG. 6. Raw data of the cos−cos decay curves of *ortho*-terphenyl at 252.4 K. The measurements have been performed parallel to the t axis for fixed values of the evolution time τ. The data sheet consists of 40 points in the t direction and 51 points in the τ direction.

EXPERIMENTAL RESULTS, ANALYSIS, AND DISCUSSION

Experiments were performed on perdeuterated *ortho*-terphenyl[1] (*13, 14*) at 252.4 K with a stability of ±0.2 K over the duration of the experiments. This is the temperature range of the supercooled liquid but still 10 K above the caloric glass transition temperature. The sample material was recrystallized in hot methanol, dissolved in acetone, and microfiltrated (pore size 50 μm) into Duran glass NMR tubes. The acetone was removed (keeping the samples for several days at 70°C under vacuum) and the sample was sealed under vacuum.

The stimulated echo experiments were performed at a deuteron frequency of 40 MHz. The pulse width for 180° pulses was 5.4 μs. The pulse sequence $(90°)_y-\tau-(90°)_y-t-(90°)_y-\Delta-(90°)_x$ was chosen to obtain the cos−cos part of the correlation function. The additional fourth $(90°)_x$ pulse was used to refocus the echo at a distance $\tau + \Delta$ after the last pulse. With this technique τ values shorter than the dead time of the receiver are available. The echo amplitude was measured for several fixed values of τ (0.2, 1, 2, . . . , 50 μs) as a function of the mixing time t. Within one measurement t was varied (equidistant on a logarithmic scale) over a range of more than four decades.

Figure 6 shows the experimental raw data (*3*). Here the cos−cos echo amplitude is plotted as a function of t and τ. The initial decay at very short mixing times ($t \approx 200$ μs) is due to multiquantum coherences (a violation of the condition $t \gg T_2$), but was recorded in order to estimate an appropriate starting point for fitting the cos−cos decay which is observed at t values between 10 and 100 ms. T_1, which in principal could lead to an additional echo damping along the t axis, is known from independent experiments to be approximately 2 s so that eventually the decay curves at the smallest τ values might be affected by T_1. The mean correlation times $\langle\tau_c\rangle$ of the ultraslow reorientation dynamics are also known from independent experiments (stimulated sin−sin echo experiments in the limit $\tau \to 0$) (*14*) so that we are able to scale the mixing time t in units of $\langle\tau_c\rangle$, the same scale as used in the simulations of Fig. 5.

Cutting off the values for mixing times below 800 μs and neglecting any influence of T_1, these raw data decay curves were fitted with the KWW function. In Fig. 7 the obtained $\langle\tau_k\rangle$ and the β_k values were again plotted as a function of the evolution time τ.

At a first glance the $\langle\tau_k\rangle/\langle\tau_c\rangle$ values behave as expected

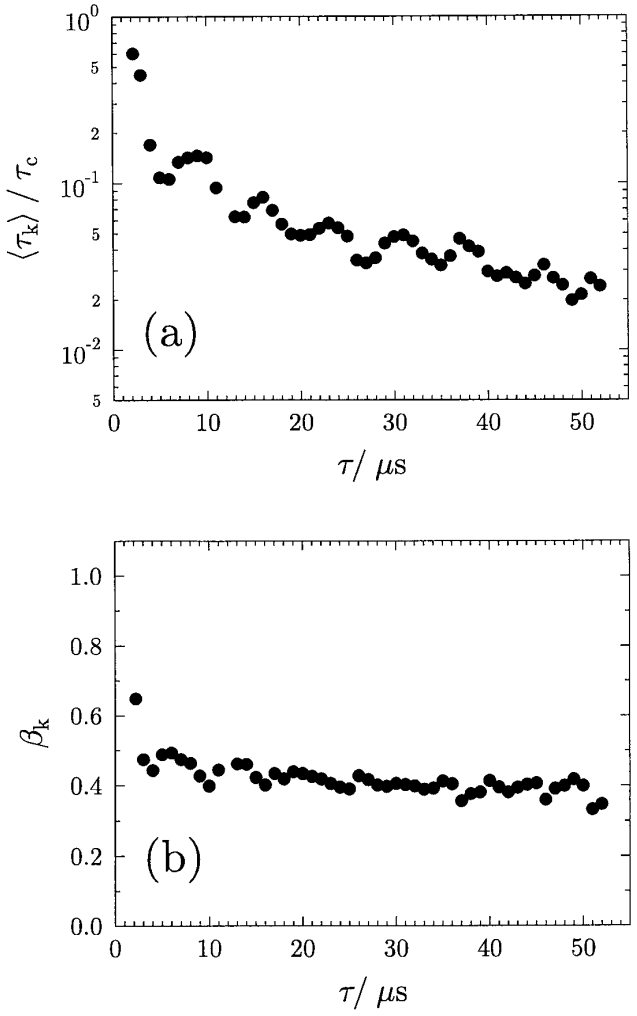

FIG. 7. The KWW parameters $\langle\tau_k\rangle$ (a) and β_k (b) versus evolution time τ, obtained for *ortho*-terphenyl at 252.4 K.

[1] The perdeuterated *ortho*-terphenyl was obtained from H. Zimmermann, Max Planck Institute für medizinische Forschung, Heidelberg.

from the simulations—they start close to unity for $\tau \to 0$ and decrease (in an oscillatory fashion) down to values of approximately 0.02 to 0.03 for τ values of 50 μs. Comparing this thoroughly with the simulations in Fig. 5 one finds that the elementary jump angle should be somewhere between 6° and 10°. But a detailed comparison also shows that there is a systematic deviation between the experimental data and the simulated curves: With increasing values of τ the experimental data cross each individual simulated curve. At small τ values they fit the simulated 10° curve but at larger τ values they are better described by the simulated 6° curve. This effect is significantly outside the scatter in the experimental data.

Comparing the β_k values with the simulated data shows no compatibility at all. The experimental β_k are found between values of 0.5 and 0.3 with no significant τ dependence, while the simulated data predict a strong oscillating behavior between values of 0.9 and 0.5. The consistancy between the results obtained from the τ dependence of $\langle \tau_k \rangle$ and the τ dependence of β_k (forced by the ansatz of our data evaluation) is clearly not found with the model used so far.

These dramatic deviations between experiment and simulation show that the assumed IFJ models are too simple to describe the dynamics of the reorientational motion in supercooled *ortho*-terphenyl. The most important simplifications might be the assumption of a well-defined ''sharp'' elementary jump angle and/or the assumption of only one well-defined correlation time. The easiest way to produce a ''smearing out'' of the elementary step in the numerical simulations is the introduction of a distribution of correlation times. In disordered amorphous systems such distributions are physically plausible and have been used in many other molecular systems to explain the observed nonexponentiality in relaxation phenomena. It is known that these distributions may become very broad so that it is convenient to use distributions based on a logarithmic time scale.

Introduction of a Correlation Time Distribution

In order to reduce the considerable amount of computer time in simulating the τ dependence of $\langle \tau_k \rangle$ and β_k, we have chosen a very simple model of distributed correlation times:

We assume a *heterogeneous* sample where different molecules have different correlation times. There should be *no spectral exchange*, e.g., single molecules keep their correlation times on the time scale of the experiment. This simplification allows for a superposition of individual echo decay curves with well-defined correlation times. Since, furthermore, the individual echo decay curves can be scaled with their correlation times, the distribution of correlation times can be introduced in a very late step of the simulation.

It is known (*15*) that in supercooled liquids correlation time distributions are usually asymmetric and very broad. With a picture of an activated random walk in a random energy landscape with a Gaussian distribution of energy barriers it is plausible to chose a logarithmic Gaussian distribution of correlation times according to

$$g(\tau_c) \propto \exp\left[- \frac{(\ln \tau_c - \ln \tau_{max})^2}{2\sigma^2} \right]. \qquad [18]$$

This distribution has a maximum at τ_{max} which is connected to the mean value (first moment) $\langle \tau_c \rangle$ via

$$\langle \tau_c \rangle = \exp\left[\frac{3}{2} \sigma^2 \right] \cdot \tau_{max}. \qquad [19]$$

The width σ of the distribution is given by $\sigma = \sqrt{\langle (\ln \tau_c)^2 \rangle - \langle \ln \tau_c \rangle^2}$ and connected with the *decadic full width at half maximum* σ_{dec} via

$$\sigma_{dec} = \log \frac{\tau^+_{1/2}}{\tau^-_{1/2}} = 2\sigma\sqrt{2 \ln 2} \log e. \qquad [20]$$

Here $\tau^+_{1/2}$ and $\tau^-_{1/2}$ are the correlation times at which the density $g(\tau_c)$ takes half of its maximum value.

The simulations are performed using 200 values of τ_c equidistant on a logarithmic scale and weighting each decay curve with $g(\tau_c) d \ln(\tau_c)$. The $\langle \tau_k \rangle$ values obtained by the Kohlrausch–Williams–Watts fits to the simulated decay curves are normalized to the $\langle \tau_c \rangle$ values (Eq. [19]) of the corresponding correlation time distribution.

Plotting the simulated $\langle \tau_k \rangle / \langle \tau_c \rangle$ and the β_k values against the evolution time τ for several values σ_{dec} of the correlation time distribution (solid lines in Fig. 8) shows the following important characteristics:

- The $\langle \tau_k \rangle / \langle \tau_c \rangle$ versus τ plots depend only very weakly on the width of the correlation time distribution. There is a small decrease in the $\langle \tau_k \rangle / \langle \tau_c \rangle$ values with increasing σ_{dec} but the shape and the amplitude of the oscillations in these plots remain characteristic for the size of the elementary jump angle.
- The β_k versus τ plots on the other hand strongly depend on the width σ_{dec} of the correlation time distribution. The strong oscillations observed for unique, well-defined correlation times become weaker and the absolute values of β_k decreases with increasing width of the distribution. If σ_{dec} exceeds two decades the oscillations in β_k have almost vanished and there is no further characteristic τ dependence observable.

Comparing the experimental data (● in Fig. 8) with such simulated curves shows that elementary jump angles in the range of 10° ± 2° are suitable to describe the observed τ dependence in $\langle \tau_k \rangle / \langle \tau_c \rangle$ (Fig. 8a) and that the width of the correlation time distribution is in the range of 1.5 to 2.0 decades (Fig. 8b). It is worthwhile to stress again that the

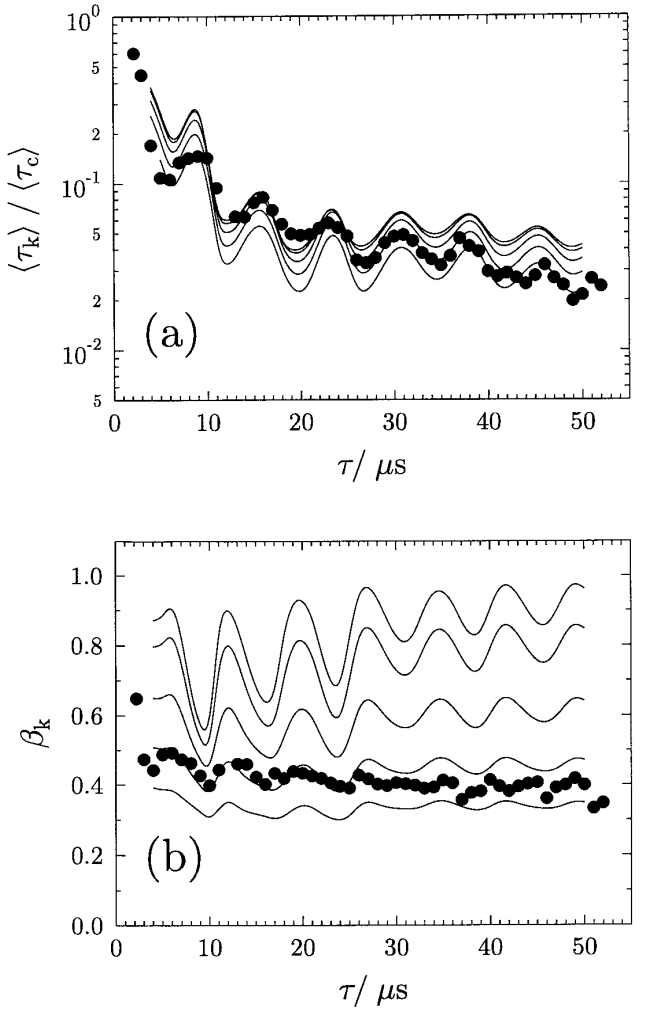

FIG. 8. The simulated KWW parameters $\langle\tau_k\rangle/\langle\tau_c\rangle$ (a) and β_k (b) versus evolution time τ for $\alpha = 10°$, heterogeneous reorientation, and several values of the decadic full-width at half-maximum σ_{dec} of the correlation time distribution (solid lines, from top to bottom: $\sigma_{dec} = 0$, 0.5, 1.0, 1.5, 2.0). The same experimental data of *ortho*-terphenyl as shown in Fig. 6 (●).

interpretation of the data is based on the simultaneous fitting of the τ dependence of both parameters $\langle\tau_k\rangle/\langle\tau_c\rangle$ and β_k.

Nevertheless, there still remain some small systematic deviations between the experimental data and the simulated curves. These deviations, outside the scatter in the experimental data, indicate that it should still be possible to improve the interpretation of the data by choosing a more sophisticated model of the elementary step of reorientation. We expect that the most successful improvement will be the introduction of a distribution of the size of the elementary jump angle, but due to the much higher effort in the simulations and due to the higher degrees of freedom in the fundamental model parameters these investigations will be the subject of future work.

CONCLUSIONS

We have introduced a treatment of experimental stimulated echo data which makes it possible to distinguish among small angle reorientation mechanisms. With the sensitivity to isotropic small angle reorientations this method is complementary to the 2D exchange spectra methods which are more suitable to resolve anisotropic large angle jumps.

We have chosen a Kohlrausch–Williams–Watts parameterization of the mixing time dependence of the echo decay curves. This approach has proven to resolve small elementary reorientation angles (below ≈25°) with a precision in the range of 1°. Furthermore the two parameters $\langle\tau_k\rangle/\langle\tau_c\rangle$ and β_k have shown different sensitivities to the size and to the ''sharpness'' of the elementary reorientational step. In the presented reorientation models we have introduced some kind of ''smearing out'' of the elementary step with the help of a distribution of correlation times. The τ dependence of $\langle\tau_k\rangle$ is highly sensitive to the reorientation angle and is insensitive to the width of the correlation time distribution while on the other hand the τ dependence of the parameter β_k is strongly related to the width of the correlation time distribution.

Applying this method to experimental data of *ortho*-terphenyl in the supercooled melt, we find a mechanism of reorientational motion which significantly differs from rotational diffusion. Elementary reorientation angles (jump angles) of 10° ± 2° are more suitable to describe the observed τ dependence of the experimental data. Using the parameter β_k we can estimate a width of the correlation time distribution in the range of 1.5 to 2.0 decades. But the precision of the presented experimental data is high enough to recognize even further deviations between experimental and simulated data. Most probably, improvements in the models used for simulations, like the introduction of a homogeneous distribution in the elementary jump angle, would account for such effects. In this sense the elementary jump angle of 10° found for *ortho*-terphenyl should be considered as a mean value, probably averaged over a distribution of several reorientation angles.

ACKNOWLEDGMENTS

We thank G. Hinze and G. Diezemann for stimulating discussions. This work was supported by the Deutsche Forschungsgemeinschaft (SFB 262).

REFERENCES

1. K. Schmidt-Rohr and H. W. Spiess, ''Multidimensional Solid-State NMR and Polymers,'' Academic Press, London (1994).
2. C. Schmidt, B. Blümich, and H. W. Spiess, *J. Magn. Reson.* **79,** 269 (1988).
3. I. Chang, F. Fujara, B. Geil, G. Heuberger, T. Mangel, and H. Sillescu, *J. Non-Cryst. Solids* **172–174,** 248 (1994).
4. K. L. Ngai, E. Riande, G. B. Wright (Eds.), ''Proceedings of the

Second International Discussion Meeting on Relaxation in Complex Systems, Alicante, Spain, 28 June–6 July, 1993,'' *J. Non-Cryst. Solids* **172–174** (1994); and ''Proceedings of the Third International Discussion Meeting on Relaxation in Complex Systems, Vigo, Spain, 29 June–11 July, 1997,'' *J. Non-Cryst. Solids,* to be published.

5. S. Wefing, Ph.D. thesis, Max Planck Institut Mainz (1988).
6. F. Fujara, S. Wefing, and W. F. Kuhs, *J. Chem. Phys.* **88,** 6801 (1988).
7. R. Zurmühl, ''Matrizen,'' Springer-Verlag, Berlin (1964).
8. S. Wefing, S. Kaufmann, and H. W. Spiess, *J. Chem. Phys.* **89,** 1234 (1988).
9. H. Sillescu, *J. Chem. Phys.* **54,** 2110 (1971).
10. Crank, ''The Mathematics of Diffusion,'' Claredon Press, Oxford (1975).
11. C. P. Lindsey and G. D. Patterson, *J. Chem. Phys.* **73,** 3348 (1980).
12. E. Helfand, *J. Chem. Phys.* **78,** 1931 (1982).
13. O. Debus, H. Zimmermann, E. Bartsch, F. Fujara, M. Kiebel, W. Petry, and H. Sillescu, *Chem. Phys. Lett.* **180,** 271 (1991).
14. F. Fujara, B. Geil, H. Sillescu, and G. Fleischer, *Z. Phys. B-Condens. Matter* **88,** 195 (1992).
15. E. Rössler, M. Taupitz, and H. M. Vieth, *J. Phys. Chem.* **94,** 6879 (1990); *Ibid* **97,** 7944 (1992).